

2017

Quantification of ventilation enhancement using the Eye CAN roof support

Michael T. Shook

Mark F. Sindelar

Hua Jiang

Yi Luo



Contents lists available at ScienceDirect

International Journal of Mining Science and Technology

journal homepage: www.elsevier.com/locate/ijmst

Quantification of ventilation enhancement using the Eye CAN roof support

Shook Michael T.^{a,*}, Sindelar Mark F.^b, Jiang Hua^b, Luo Yi^b^a Burrell Mining Products, Inc., New Kensington, PA 15068, USA^b Department of Mining Engineering, West Virginia University, Morgantown, WV 26506, USA

ARTICLE INFO

Article history:

Received 6 June 2016

Received in revised form 1 September 2016

Accepted 18 October 2016

Available online 7 December 2016

Keywords:

Standing roof support

CAN

Ventilation

Load-displacement

Eye CAN

ABSTRACT

Convergence of roof and floor in underground mine openings is a common occurrence. This convergence not only adversely affects the ability of workers, equipment and supplies to travel through the mine, it also reduces the effectiveness of the mine ventilation system, which is essential for the dilution of methane gas and airborne respirable dust. While installing secondary standing supports to control floor and roof convergence, such supports, by nature, partially obstruct a portion of the airway. These added obstructions inhibit the ability of the ventilation system to operate as efficiently as it could by increasing the resistance in and reducing the cross-sectional area of the airway. This study introduces and demonstrates the benefits of The Eye CAN™ standing roof support, which controls floor and roof convergence and is less obstructive to air flow than conventional wooden cribs. Laboratory findings show that the normal resistance of a supported lined airway is reduced by using this new product from Burrell Mining Products, Inc., while providing the same roof support characteristics of an established product—The CAN®. Load vs. displacement curves generated from laboratory tests demonstrated that this new product behaves with the same roof support characteristics as others in The CAN product family. Ventilation data gathered from a simulated mine entry was then used for computational fluid dynamics (CFD) modeling. The CFD analysis showed an improvement with The Eye CAN vs. other accepted forms of standing roof support. This proof-of-concept study suggests that, when using this new product made by Burrell Mining Products, Inc., not only will the convergence from the roof and floor be controlled, but airway resistance will also be reduced.

© 2016 Published by Elsevier B.V. on behalf of China University of Mining & Technology. This is an open access article under the CC BY-NC-ND license (<http://creativecommons.org/licenses/by-nc-nd/4.0/>).

1. Introduction

One of the basic elements of underground mining is the necessity to support the mine roof. It is well-known that easier reserves have been mined so that today's underground mines present challenging conditions. Factors influencing roof support decisions include mine depth, mining method, overburden composition, and agency regulations. Mining engineers, therefore, have to balance three objectives: safety, engineering, and cost.

While safety is obviously paramount, and engineering often complements safety, the cost effectiveness of any product, method, or device warrants additional consideration in today's harsh business climate. Avenues for adaptation and improvement are found at the intersection of the three objectives.

Burrell Mining Products, Inc., developed The CAN® cribbing system of standing roof support two decades ago in the shadow of the

Valley Camp Mine located in New Kensington, Pennsylvania. When Valley Camp opened in 1910, it relied on timbering for roof support. This historical reference to a room and pillar drift mine in a 1.82 m seam is important since it illustrates the early origins of the evolution in standing roof support and recognizes that one of the most basic forms, wooden cribs, is still in use after a century.

Mining engineers of the Valley Camp era could not visualize four-mile longwall panels with extensive bleeder entries, their associated ventilation plans and, therefore, their critical roof support requirements. Nor could they have anticipated the ever-expanding regulatory requirements that today include roof control and ventilation plans, as applied to longwall coal mining. To address ground control issues, a number of primary strategies are employed for standing roof support in longwall bleeder entries, including wooden cribs, pumpable cribs, and The CAN cribbing system.

Since its introduction, The CAN, manufactured exclusively by Burrell Mining Products, Inc., has been a popular choice for roof support, especially in challenging areas of underground coal mines

* Corresponding author. Tel.: +1 724 339 2511.

E-mail address: mshook@burrellinc.com (M.T. Shook).

where convergence is very pronounced, as in bleeder entries. Convergence, however, not only affects roof support but also restricts ventilation both by reducing the cross-sectional area of the entry and by introducing non-uniformities, such as rib sloughage, that change the air flow dynamics.

Recent directives from the Mine Safety and Health Administration (MSHA) amplify the necessity to maintain open access and sufficient air flow in bleeder entries. Since standing roof support intrinsically obstructs a portion of the cross-section of any entry where it is installed, reducing the impact on ventilation from the standing roof support furthers the objective of improving ventilation while maintaining support for the roof.

Burrell Mining Products, Inc., has added a new member to The CAN product family—The Eye CAN. This paper describes the motivation for developing The Eye CAN (patent pending), examines how this new product has been evaluated as a standing roof support, and introduces initial findings of the current study to evaluate its efficacy as a less-obstructive component to the ventilation system.

2. Background

The CAN is recognized as the most stable of the deformable concrete supports and “remains the dominant form of tailgate support,” particularly in mines of the Western United States [1,2]. As such, it is a prime candidate for enhancements that would allow it to be more transparent to air flow while still maintaining the same roof support capabilities for which it has earned its reputation.

All products of The CAN family, including The Eye CAN, consist of a thin cylindrical steel shell filled with aerated concrete. As part of a standing roof support system, The CAN is placed axially in a mine entry, and the space between the top of The CAN and the mine roof is packed with wood timbers [3]. Fig. 1 depicts a typical installation.

Establishing full contact between the roof and the top of the support is necessary to obtain full benefit from the support system [4]. Barczak and Tadolini have shown the stiffness of the system with the following equation [2]:

$$K_{system} = \frac{K_{crib}K_{CAN}}{K_{crib} + K_{CAN}} \quad (1)$$

where K is the stiffness in kips/in. A study by Gearhart and Batchler investigated a number of relevant parameters that affect performance of The CAN, including the species of wood. With varying K_{crib} , the same researchers investigated multiple layers of cribbing, as well as the errant procedure of not completely filling the interface between The CAN and mine roof with cribbing [5]. They found decreased performance in terms of stiffness for both scenarios.



Fig. 1. Installed The CAN® roof supports in mine entry, 0.46 m diameter.

Using a single layer of closely packed and appropriate timbers is one of the recommended installation guidelines [4].

Thus, when properly installed, The CAN has never failed as a standing roof support and over one million have been installed worldwide. Published reports of possible “drawbacks” for using The CAN list only simple errors that happen during improper installation [4–6]. The product itself has not been criticized. It is capable of withstanding in excess of 50.8 cm of vertical convergence while simultaneously accommodating 38.9 cm of displacement in the horizontal direction [5]. As The CAN takes load, it exhibits elastic behavior with a steep load-displacement curve dependent on the stiffness of Eq. (1). The support then yields longitudinally at a load amplitude that is a function of The CAN diameter. Larger diameters are positively correlated to more load-bearing capacity, as shown in the chart of Fig. 2. Conversely, while pumpable cribs may initially exhibit a high stiffness, significant load shedding occurs so that post-failure capacity is commensurate with that of wood cribs [1]. Wood cribs, then, become the baseline for comparison.

This elastic-plastic behavior and the characteristic curve define what constitutes The CAN roof support system. Since its introduction, over 130 tests have been performed by the NIOSH Mine Roof Simulator (MRS) in Pittsburgh, Pennsylvania [5]. The performance characteristics of The CAN are well established, and mines using The CAN for standing roof support rely on a standard of performance defined by this load-displacement curve so that any new The CAN product must meet these requirements. Note that tests were conducted by independent laboratories using imperial units to remain consistent with historical test data for The CAN product line, such as the curve shown in Fig. 2.

If The CAN provides excellent roof support, then why would anyone want to modify it? Consider next the motivation for an enhanced standing roof support. At the end of 2013, MSHA issued Program Policy Letter (PPL) No. P13-V-12, “to provide consistency in the application of the standards with regard to travel, examination, evaluation, and means for determining the effectiveness of bleeder systems” [7]. The guidance provided therein was in response not only to the noted explosion at the Upper Big Branch Mine in April, 2010, but also to increasing numbers of both ignitions/explosions and imminent danger orders resulting from conditions in longwall bleeder systems. A primary concern mentioned in the PPL was safe access to the bleeder entries for both inspection and evaluation. While the accumulation of water is a separate issue outside the scope of this paper, the occurrence of roof falls is germane. Roof falls and convergence both contribute to reductions in cross-sectional area, which negatively affects ventilation and can also create obstructions to travel for personnel.

Since the use of standing roof supports inevitably obstructs some of the cross-sectional area in the locations where the supports are placed, the objective would be to somehow allow more

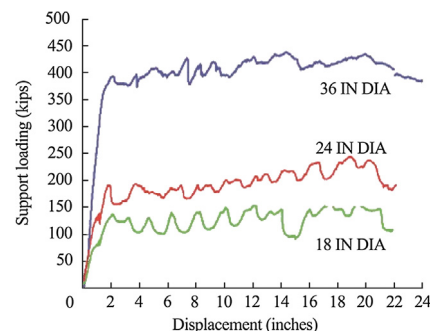


Fig. 2. Load-displacement curves for 45.72, 60.96, and 91.44 cm diameter The CANS® (Note: 1 kip = 0.453 metric ton; 1 in. = 2.54 cm).

of the ventilation air to flow around or through the support. This concept led to development of The Eye CAN.

3. The Eye CAN

The Eye CAN is manufactured with apertures located axially through the shell so that, when the centerline of the apertures is placed in alignment with an air flow, such as in a bleeder entry, the air can flow through the “eye,” thereby reducing overall restriction in the entry. A 55.88 cm diameter Eye CAN is shown in Fig. 3, with appropriate top capping with wood cribs.

For example, in a 4.88 m wide entry with a 2.13 m mining height, the use of two The Eye CAN supports measuring 55.88 cm in diameter would obstruct 22.92% of the cross-section, whereas two The Eye CAN supports with two 15.24 cm diameter apertures would only obstruct 22.57% of the cross-section, resulting in an improvement to cross-sectional area of 0.35%. Assuming 0.31 m of convergence, The Eye CAN then returns 0.41% of the cross-sectional area. It should be noted that these cross-sectional area calculations are made at the full diameter of The Eye CAN. While each The Eye CAN is set in compliance with the roof control plan of the mine, a double row on 238.76 cm centers is representative, whereas 198.12 cm centers would be required for wooden cribs so that the contribution of the “eye” is understated when considering solely cross-section.

The geometry of The Eye CAN presents a number of advantages for ventilation. Considering the cross-sectional area of an entry at the location of the roof support, The Eye CAN provides less obstruction than other types of roof support, such as four-point cribs. Furthermore, the round steel exterior provides a smooth surface that promotes air flow around The Eye CAN, whereas four-point cribs are known for creating turbulence. Thus, to demonstrate effectiveness, The Eye CAN must demonstrate the same roof support capabilities and standards of previously developed supports of The Eye CAN product family, and demonstrate a reduction in resistance to ventilation air flow better than can be obtained from only the cross-section calculations.

Burrell Mining Products, Inc., conducted some evaluations of the newly developed The Eye CAN, the classic roof support The Eye CAN, and traditional four-point wood cribs.

4. Load-bearing evaluation

A unique feature of The Eye CAN is how its strength increases as it bears load, while deforming along the axis of load. To confirm that The Eye CAN would perform similarly to The Eye CAN, the load-displacement curve had to exhibit the same elastic-plastic charac-



Fig. 3. 55.88 cm diameter The Eye CAN® at NIOSH mine roof simulator (MRS).

teristics. That is, for The Eye CAN, as the support initially takes load, the response is elastic as it rapidly builds to yield, then becomes plastic as a strain-hardening phase occurs.

A total of 17 samples of The Eye CAN were tested: 12 at TÜV Rheinland Industrial Solutions, Inc., and 5 at the Mine Roof Simulator (MRS) at the NIOSH Pittsburgh Research Lab. Based on the results, the Research & Development (R&D) Department at Burrell Mining Products, Inc., made appropriate modifications to the design prior to each round of additional testing.

Vertical and biaxial loads were applied to a variety of The Eye CAN configurations during the research and development process. In all cases, each test employed The Eye CAN that maintained the recommended minimum aspect ratio of 5:1 [5]. A concentration of effort was placed on the popular 55.88 cm diameter, which the R & D department found to be more convenient for mines employing rail haulage than the 60.96 cm diameter.

Fig. 4 shows load-displacement curves for two different heights of the 55.88 cm diameter The Eye CAN, each with two 15.24 cm ports. This diameter, in addition to being popular, represents a conservative case for The Eye CAN support (see Fig. 2). Fig. 5 shows a comparison between The Eye CAN subjected to vertical loading and The Eye CAN subjected to both vertical and shear loading at a ratio of 2:1.

In addition to the roof support capabilities, another important consideration in the design of The Eye CAN was the ability of the “eye” itself to remain intact (open) as long as possible as the support yields under load. Since the purpose of the eye is to allow for air flow, distortion of the eye, while maintaining as much cross-section as possible, was acceptable, as shown in Fig. 6. Obviously, as convergence of the entry would continue, in its limiting case, the eye would become closed. However, by this time, the bleeder entry would have been sealed, eliminating the need for travel by mine personnel and for ventilation.

The load-displacement curves for The Eye CAN are commensurate with that for The Eye CAN.

5. Ventilation study

The load-bearing characteristics of The Eye CAN versus four-point cribs are not one-to-one. Typical roof support plans per running 30.48 m of entry will use 30 four-point cribs, rated at 40 tons, versus 26 The Eye CAN supports, rated at 80 tons. Therefore, even though the same number of four-point cribs and The Eye CAN supports were compared for the ventilation study, this was a conservative approach since more wooden cribs would be required to achieve a similarly calculated amount of roof support. The goal of the ventilation study was to gather data about the performance of The Eye CAN, The Eye CAN, and wood crib support systems for use in CFD. The CFD simulations have been shown to be effective in modeling ventilation phenomenon in mine entries when experimental data is used to validate the model [8].

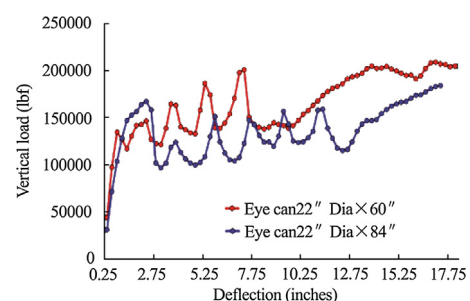


Fig. 4. Load-displacement curves for 55.88 cm The Eye CAN® support (Note: 60 in. = 152.4 cm; 84 in. = 213.36 cm; 1 lbf = 0.453 kg).

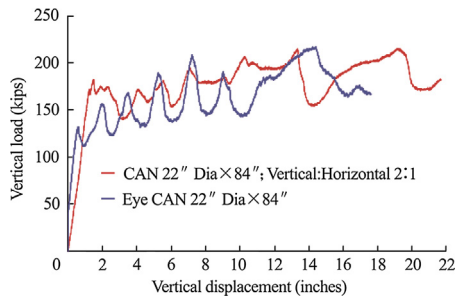


Fig. 5. Load-displacement curve comparing 22 in. (55.88 cm) diameter The CAN® and The Eye CAN (Note: 84 in. = 213.36 cm; 1 kip = 0.453 metric ton).



Fig. 6. The Eye CAN® with 45.72 cm vertical displacement (convergence), area of "eye" maintained.

A 21.34 m long simulated bleeder entry, characterized by low velocity air movement with some leakage and obstructions, was constructed at a warehouse. The sides and top of the simulated entry consisted of brattice cloth loosely fastened to wooden frames to simulate the imperfect ribs and top of a coal mine; the floor was the concrete floor of the warehouse. Fig. 7 shows the simulated entry which was 4.88 m wide and 2.13 m tall.

Exhaust ventilation was provided by a Master MAC-42-BDF shop fan. The differential pressures obtained were small and below the resolution of the manometer—an unsurprising result since obtaining these readings in working coal mines is often problematic.

Air leakage was controlled as best as could be expected given the nature of the setup. The largest concern was the seal at the fan, which had to be secured after each change in the type of roof support. Typical roof support configurations consisted of 14, 8, and



Fig. 7. Simulated mine entry.

6 four-point crib sets; 14, 8, and 6 The CAN supports; and 8 and 6 The Eye CAN supports, all in parallel rows. Six configurations were arranged for the ventilation study; the remainder are for future work.

Air velocity readings were taken at three locations, 1.83, 9.14, and 18.29 m respectively, as measured from the intake end. At each location, 35 air readings were measured on a 7×5 grid, equally spaced along the width and height, respectively, with a CEM DT- 8880 hot wire anemometer. The velocity measurement range of the anemometer is from 0.10 to 25 m/s with a resolution of 0.01 m/s. Its ability to measure low air velocity is important for this study since air velocity in entries where the standing supports are used is normally low. All readings were taken by a certified mine foreman. Fig. 8 depicts The Eye CAN in the simulated entry with the measuring device used to assure consistency of location when taking readings with the hot wire anemometer. The geometries of the layouts are shown in Fig. 9.

Three pairs of data (six sets) generated for the standing roof support configurations, shown in Fig. 9, were used for CFD analysis. The first two pairs compared wood cribs to The CAN and the third pair compared The CAN to The Eye CAN.

CFD simulations were conducted with Cradle SC/Tetra 12.0 (Software Cradle Co., 2016). Three steady state simulation analysis cases were performed. Two were based on the simulated mine experiment readings. The third considered the use of The Eye CAN under the same conditions. A geometric model representing the three cases was built according to the design measurements of the full-scale simulated entry.

The geometry and associated boundary conditions are illustrated in Fig. 10. Air entering the simulation domain is depicted by an inlet with a natural inflow condition. An outlet with a negative static pressure was placed at the fan. All the other boundaries within were defined as walls. In order to model each case, eight supports were placed into the entry, seen in Fig. 10, with The Eye CAN depicted.

For the first two models, the average air velocities in the entry cross-section area were examined for the purpose of validation. After the validation process, the prediction case used the same simulation parameters to study the air flow distribution in the entry using The Eye CAN support.

Fig. 11 and Table 1 show the simulated and experimental entry cross-section velocity contours and average velocities. The CFD simulation cases agreed within $\pm 5\%$ of the experimental data. Therefore, a comparison between the results with the laboratory experiments indicates that the CFD model can accurately model and represent the simulated mine entry and reinforces the appropriateness of the boundary conditions.

Using the same number of The CAN supports instead of cribs, the air flow rate is higher. The effect is more pronounced when recognizing that eight The CAN supports are roughly equivalent in



Fig. 8. The Eye CAN® (right) and "measuring stick" (left) (Note marks on floor).

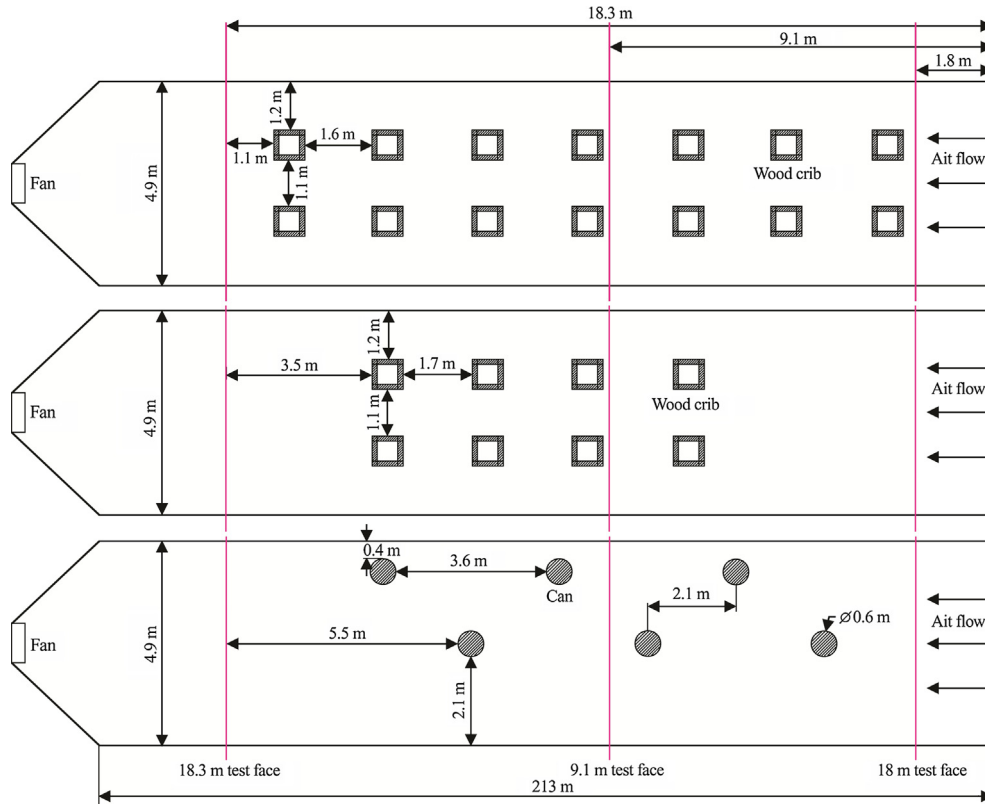


Fig. 9. Layouts for CFD modeling corresponding to the simulated mine entry experiment.

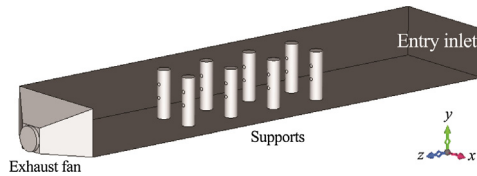


Fig. 10. Geometric and locations of boundary conditions for CFD model.

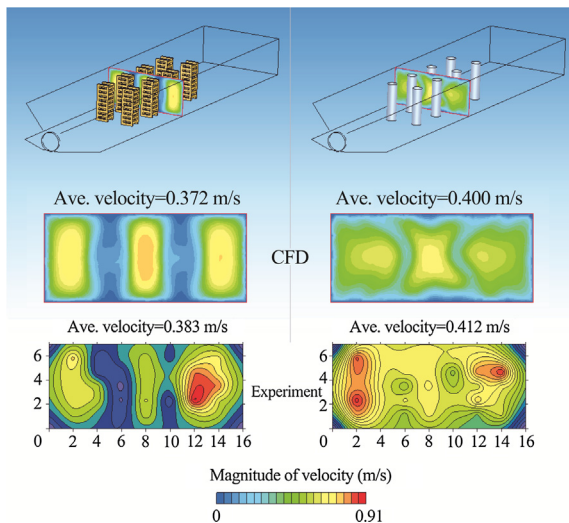


Fig. 11. Velocity contours of crib supports (left) and The CAN® supports (right) for CFD (up) and experiment (down) study.

roof support capacity to 14 four-point cribs. In this case, the flow rate has been increased by almost 30%. This is mainly due to the smoother surface and less contact surface area directly facing

opposite the direction of air flow. As seen from the last pair of data, by using The Eye CAN supports in the entry, the air flow velocity is 0.22% higher than using traditional The CAN supports.

Table 1 shows the flow rates determined from the air velocity measurements at the three test locations for the cross-section (Fig. 9) for each of the experiments. Due to air leakage, some errors are believed to exist in the first data set of Experiment No. 1, so this data was omitted. Otherwise, the flow rates used in the analysis should be representative of the actual conditions of the scenario and comparable to those in standing entry between two mine longwall gobs. Comparing the flow rates, the ventilation impact of the different supporting structures is evident.

To obtain a quantitative assessment of ventilation performance for each of the supporting methods, CFD modeling technique is used where it is not practical to collect data by laboratory experiment. Airway resistance (R) and friction factor (K) are back-calculated from the pressure differences (H) obtained from the CFD simulations. The resulting R and K are used to assess the ease of mine ventilation through an airway and are defined by Eqs. (2) and (3) [9].

$$R = \frac{H_l}{Q^2} \tag{2}$$

$$H_l = \frac{KOLQ^2}{5.2A^3} \tag{3}$$

where R is the resistance, $\text{Pa s}^2/\text{m}^8$; H the head loss, Pa ; Q the flow rate, m^3/s ; K the friction factor, $\text{kg s}^2/\text{m}^4$; O the perimeter of the entry, m ; L the length between two panels, m ; and A the cross section area, m^2 .

The head loss is obtained from the pressures measured at two airway cross-sections (P_1 and P_2 in Fig. 12) in the CFD model. The flow rate is determined from the average air velocity (V in Fig. 12).

Table 1
Flow rates and velocity data for the experiments and CFD simulations.

| Exp. pair No. | Support method | Cross section distance from the air inlet point | | | Exp. | CFD |
|---------------|---------------------|---|---------------------------|----------------------------|--------|--------|
| | | 1.83 m Flow rate (m/s) | 9.14 m Flow rate (m/s) | 18.29 m Flow rate (m/s) | | |
| 1 | 14 cribs | 35.02 | 19.41 | 36.86 | 0.3209 | |
| | 14 CAN | 48.06 | 52.11 | 49.19 | 0.4446 | |
| 2 | 8 cribs | 42.90 | 43.03 | 42.85 | 0.3832 | 0.3721 |
| | 8 CAN | 45.96 | 48.98 | 43.38 | 0.4117 | 0.4004 |
| 3 | 6 CAN staggered | 43.00 | 46.97 | 45.14 | 0.4021 | |
| | 6 Eye CAN staggered | 47.35 | 45.73 | 50.88 | 0.4284 | |

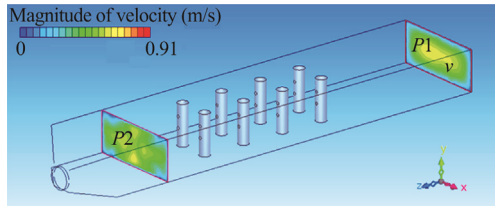


Fig. 12. CFD simulation results and parameter locations.

Table 2
Atkinson resistance and friction factor results for three cases.

| Parameter | Support method | | |
|---|----------------|-------------|-------------|
| | Crib | The CAN | Eye CAN |
| P_1 (Pa) | -1.1249E-02 | -2.0922E-02 | -2.2922E-02 |
| P_2 (Pa) | -4.7459E-02 | -4.2123E-02 | -4.4031E-02 |
| H_i (Pa) | 3.6210E-02 | 2.1201E-02 | 2.1109E-02 |
| v (m/s) | 0.3718 | 0.3958 | 0.3967 |
| Resistance (Pa s ² /m ⁸) | 2.6047E-02 | 1.3455E-02 | 1.3337E-02 |
| Friction factor ($\times 10^{10}$) | 10841024.3 | 5600249.9 | 5543490.6 |

Table 2 shows that, by using either The CAN or The Eye CAN support, the resistance and friction factor is only 35% compared to wood crib supports. Smaller resistance makes it easier for ventilation air to pass through an entry. In a comparison between The CAN and The Eye CAN, the parameters are very close. The air velocity in The Eye CAN supported entry is 0.22% larger than The CAN supported entry. Although appearing numerically small, the experiment was performed with a limited number of standing roof supports in a 21.34 m long simulated entry with low velocities and known leakage. Since the resistance and friction factor indicate that the ventilation performance of The Eye CAN is an improvement versus The CAN, the cumulative effect is expected to be larger in environments such as a full-sized bleeder entry.

6. Conclusions

Initial laboratory tests of patent-pending The Eye CAN demonstrate that it has roof support characteristics commensurate with The CAN product family, and CFD modeling shows a reduction in

resistance of 0.22% to air flow when using The Eye CAN versus The CAN. Additionally, the traditional The CAN shows a 35% improvement in ventilation when compared to using four-point wood cribs. Small modifications that provide cumulative benefits are often more cost effective than making large changes. This proof-of-concept study shows the efficacy of The Eye CAN. Future work includes an application to quantify the overall ventilation improvement in a bleeder entry.

Acknowledgments

The authors would like to thank the many individuals who assisted with this two-year project. Tim Batchler at the NIOSH Mine Roof Simulator provided technical support. Kris Lilly of Red-bone Mining lent a truckload of cribbing for the experiment. Don Abel of Burrell Mining Products, Inc., supervised fabrications, coordinated movement of materials, and modified The Eye CAN designs as required. Jim Barbina, PA Operations Plant Manager, and his crew constructed the simulated mine entry and tirelessly reset roof supports for each of the thirteen test configurations.

References

- [1] Software Cradle Co. SC/Tetra Software. Software Cradle Co., Ltd.; 2016 <<http://www.cradle-cfd.com/products/sctetra/>>.
- [2] Barczak TM, Tadolini SC. Standing support alternatives in western longwalls. *Min Eng* 2006;58(2):10.
- [3] Burrell Mining Products. The CAN®; 2012. <<http://www.burrellinc.com/the-can/>>.
- [4] Barczak TM. Mistakes, misconceptions, and key points regarding secondary roof support systems. In: *Proceedings of the 20th international conference for ground control in mining*. Morgantown, WV: West Virginia University; 2001. p. 347–56.
- [5] Gearhart DF, Batchler TJ. Aspect ratio and other parameters that affect the performance of Burrell CAN roof supports. In: *Proceedings of the 31st international conference for ground control in mining*. Morgantown, WV: West Virginia University; 2012. p. 9.
- [6] Barczak TM, Tadolini SC. Pumpable roof supports: an evolution in longwall roof support technology. *Trans Soc Min, Metall, Expl* 2008;324:19–31.
- [7] MSHA. Examination, evaluation, and effectiveness of bleeder systems. Program Policy Letter No. P13-V-12. Mine Safety and Health Administration; 2013. p. 7.
- [8] Wala AM, Yingling JC, Zhang J, Ray R. Validation study of computational fluid dynamics as a tool for mine ventilation design. In: *Proceedings of the 6th international mine ventilation congress*. Pittsburgh, PA: SME; 1997. p. 519–25.
- [9] Howard LH, Jan MM. *Mine ventilation and air conditioning*. 3rd ed. New York, NY: Wiley-Interscience; 1997.